International Forum on Aeroelasticity and Structural Dynamics
IFASD 2019
9-13 June 2019, Savannah, Georgia, USA

CHARACTERIZING A MULTI DELTA WING FOR AEROELASTIC WIND TUNNEL EXPERIMENTS

Jonas Zastrow[1]

[1]DLR Institute of Aeroelasticity
Goettingen, Germany
jonas.zastrow@dlr.de

Keywords: double delta wing, vortex lift, grid adaptation, buffeting

Abstract: The vortical flow over swept wings with several leading edge separations bears a number of challenges for the proper design of the planform and the efficient control during the flight. Leading edge vortices function as the major lifting mechanism for combat aircraft and depict the aircraft's moment coefficients as well. The flow is either unsteady or a least quasi-steady as soon as the vortices are formed, but never steady.

Even though the mechanisms of the vortical flow and its effects on the aircraft's forces and moments are well understood, their prediction is still not precise enough. Several failures of jet prototypes occurred in the past, which were accounted to unexpected vortex shifts and thus load changes, or to fatal vortex structure interaction. Resolving the flow topology over combat aircraft configurations numerically is not feasible, yet. Due to the unsteadiness time resolved calculations are needed in order to reveal all important aspects of the flow, which demands more CPU-capacities than are available at the moment. Thus only selected flow cases can be resolved. RANS-calculations dampen many effects significantly, which distorts the observed planform characteristics. Additionally the different positions of the vortices throughout the flight regime compromise efficient grid development. As a consequence wind tunnel experiments with time resolved measurements are needed and must be developed carefully, since they are very costly.

The trend shows that modern combat aircraft planforms provide multiple leading edge vortices, which take over specific functions such as stabilization, distribution or manoeuvring. Such a next generation planform has been developed by the DLR Institute of Aeroelasticity as well. Two wind tunnel test campaigns are planned with a semi-span model. A preliminarily selected sensor placement is crucial for the success of the measurements and additionally the structural layout must be constructed very carefully in order to ensure the structural integrity of the model throughout the entire flight regime. The flow topology of the aircraft model features a two-stage vortex systems, which leads to severe load changes between subsonic and supersonic velocities. Furthermore vortex-vortex interaction and vortex-structure interaction shall be characterized during steady positions, during pitching motions and during manoeuvres.

The aforementioned tasks have been and are still prepared by numerical simulations with the DLR TAU-code. An angle of incidence and Mach-number matrix gave a rough characterization of the new model planform. Strong gradients in the coefficient slopes show points of interest and convergence problems show possible critical points. In order to improve the resolution of the flow topology the TAU grid adaptation module was used and up to three adaptation stages were implemented. This resulted in resolving secondary separations, tertiary separations

and feeding sheets effectively. The newly developed model with its unique vortex topology poses very interesting characteristics and could provide a new base for modern combat aircraft developments. The structural layout and sensor placement is in progress and accompanied by time resolved simulations. These efforts should improve the quality and the efficiency of the currently planned wind tunnel experiments at the DLR and furthermore the derived routines for the numerical preparation of experiments can be adopted by succeeding projects as well.

1 INTRODUCTION

The sole usage of CFD is not enough to characterize and overcome most fluid mechanical challenges, yet. Thus the demand for experiments to support development processes is still high. Especially wind tunnel experiments are consuming a lot of personal and financial resources. In respect to the resulting risks, which wind tunnel experiments bear, the DLR Institute of Aeroelasticity focuses strongly on sophisticated preparations. In hindsight of the investigation on vortex dominated flows over a semi-span combat aircraft model an extensive use of CFD is required beforehand. The placement of pressure transducers on the model as well as its structural layout depend on the chosen flight regime and on the reduced frequencies. The latter two must be chosen according to the numerical results, which incorporate not only steady, but also unsteady simulations. The current project features a planform design that is based on a double delta (fig. 1). Its geometry is enhanced by a diamond fillet and a chined fuselage, which leads to a two stage vortex system. This leads to different flight characteristics and load distributions between subsonic flight and supersonic flight. The vortex topology in the supersonic velocity regime is with its two distinct leading edge vortices rather simple (fig. 2), whereas the subsonic flight regime incorporates three leading edge vortices of whom two interact strongly and the other one is not stabilized and thus a candidate for feeding sheet tearing and early vortex breakdown (fig. 3).

The borders of well handling are depicted by critical points, which are resembled through strong gradient changes in the coefficient matrices. Those critical points are usually connected to vortex breakdown on a jet configuration. When the breakdown reaches the trailing edge the suction force on the planform's surface starts to subside. The breakdown will move along the chord towards the leading edge, until the leading edge vortex has fully diminished. This and the unsteady movement of the breakdown along the chord during the procession from trailing to leading edge leads to severe load changes. In real flight scenarios these load changes can lead to a loss of manoeuvrability, which would be fatal during combat or would lead to complications during take-off and landing under strong cross winds. Hence a thorough characterization of the flow topology throughout the flight regime and the evaluation of fluid structure interaction therein are necessary.

Primary leading edge separations on swept wings tend to show strong pressure and strong velocity gradients and are additionally large compared to the wing's geometry. However, it is a laborious task to resolve phenomena of smaller degree such as the feeding sheets or the secondary separations consistently throughout the flight regime and if wished to do so, this leads eventually to a very large number of numerical grid points. The DLR-TAU solver provides a grid adaptation technique to overcome the usage of large numerical grids, while still resolving the flow topology properly. On the contrary the adaptation technique can provide an even more detailed resolution of the flow topology, compared to a conventional grid of the same size.

The following chapters provide an overview of the new wind tunnel "devil"-model flow topology ("designed experiments on vortex induced loads"). Furthermore its resolution with the grid

adaptation technique is shown and explained. Consequently aeroelastic challenges are derived from the numerical simulations with the TAU-solver.

2 WIND TUNNEL MODEL GEOMETRY

Cut down to the point the description of the geometry is as follows: The semi-span wind tunnel model has a double delta planform of $75°/45°$ sweep with a diamond-shaped fillet and a cosine-shaped chined nose featuring an ogival planform. The wing tips are cropped and the trailing edge sweep is $10°$. Last but not least the profiles of the wing's segments are all of parabolic shape and end on radii at the leading edges, which are constant along the span, while measuring 1% of the total half span (fig. 4, 5 & 6).

The selection of those geometrical features is based on the task to create an aircraft planform, which can operate with high agility in the subsonic, transonic and supersonic flight regime. Additionally the shapes are adapted towards a low radar signature without compromising the aerodynamic function of the specific section. In fact many design aspects favour both objectives in the same fashion. Some examples are the small radii at the leading edge, the perpendicular trailing edge and the distinct kinks between the different planform sections. The small radii suppress very likely tertiary separations, while they weaken the influence of secondary separations [1]. Furthermore they increase the relative vortical lift increments of the total lift and lead to an earlier separation at lower angles of incidence [2]. The perpendicular trailing edge grants benefits for numerical grid generation and is not likely to pose convergences issues in contrast to a round trailing edge. Last but not least the kinks introduced by the diamond fillet define a distinct onset for the leading edge separations [3]. As a result Reynolds-number effects are less pronounced, thus the kinks facilitate a more effective pressure transducer placement on the wind tunnel model.

Contradicting the design, in hindsight of a low radar signature, are for example the ogival planform of the nose, the cosine shaped cross section of the nose and the parabolic wing profiles. Whereas the planform of the nose could have been a straight edge with the same sweep of $75°$ as the steeper diamond leading edge without compromising the function of the vortex system, there is no detrimental drawback by keeping the classical ogival nose planform in wind tunnel experiments, therefore it simply was not changed. However, the cross-section in shape of a cosine is indispensable in order to achieve the desired stability during yaw and pitch manoeuvres and creates one of the key elements of the overall aerodynamic system [4]. Whereas most former experiments on leeside flows over combat aircraft featured flat plates for profiles and often no contoured leading edges the current model is equipped with both, parabolic profiles and round leading edges. The parabolic shapes are an easy estimation to create profiles suited for supersonic cruise [5], which is part of the demanded flight envelope. Since the slope of the parabolic surface gradient is nearly constant, shock movement is believed to occur rather gradually than volatile. As a result the unsteadiness around the shocks might decrease, which would be favourable for numerical calculations as well as resolving the shock topology during the experiments.

3 GRID ADAPTATION TECHNIQUE

Before the aerodynamic topology of the semi span model and thus sources for buffeting are introduced, the grid adaptation technique shall be explained shortly.

A sophisticated mesh construction is crucial in order to resolve fluid mechanical phenomena correctly. The flow topology over swept wings with multiple leading edge separations is char-

acterized by spots of strong gradients, which are inconsistent throughout the flight regime. A proper resolution would demand a numerical grid that is manually refined in all those potential areas and would thereby lead to a large number of cells. Whereas this approach is feasible for transport aircraft, which are usually characterized by a more or less 2-dimensional flow, it is rather not suited for the highly 3-dimensional flow topologies of combat aircraft. Especially tertiary or even secondary separations can be affected by the orientation and distribution of the cells, thus those relatively small topological elements may be weakened by numerical diffusion. Consequently the grid generation has impact on the overall flow topology.

An approach to those effects is the grid adaptation technique, which is implemented in the DLR TAU-code. Working with grid adaptation is based on several successive numerical calculations, whose converged solutions are analysed in hindsight to grid areas in need of a better resolution [6, 7]. There are many criteria for refinement, which can be chosen individually for each refinement step. The refinement algorithm can either search for vortex indicators such as kinematic vorticity, the Q-criterion and the Lambda-criterion or it can be used to look for large differences or gradients in the field parameters. The vortex indicators use strictly defined thresholds, which depict whether the algorithm marks the looked on area for refinement or not. This leads eventually to difficulties in vortex dominated flow with leading edge separations emerging from sharp edges. The secondary and tertiary separations, which can be expected, are weak compared to the primary separations. Depending on the chosen threshold, this results in either too many cells or too few cells that are marked for refinement. Thus the usage of vortex criteria leads either to a grid which has too many cells or does not resolve the leading edge separations of higher order properly.

Consequently schemes that search for differences or gradients should be used in order to resolve the flow topology with phenomena of higher order. The benefit of the grid adaptation technique is, that only one initial grid is needed for all calculations. This can be achieved, when a grid addresses the properties, which all flows show in the desired flight regimes. The most common phenomena chosen to resolve in a uniform manner are the leading edge suction, the boundary layer and the tip vortex. In other words the initial numerical grid provides a fixed surface and boundary layer resolution, but a coarse tetrahedral mesh, which has to be refined. In this set-up a start with gradient based adaptation should be favoured, since the higher grid resolution near the surface can be accounted for and thus the onsets of secondary and tertiary separations are refined as well as the stronger primary separations in the coarser grid area well above the suction surface. The more adaptation steps are done the more the difference scheme becomes feasible, since this scheme reduces possibilities of cell clutter in contrast to the gradient based method.

The usage of grid adaptation provides a fast procedure to fully resolve any flow topology, whose details are unknown a priori. At least two effects of the adaptation technique must be controlled, in order to maintain the validity of the results on adapted meshes. First of all the minimum cell size has to be restricted, otherwise the turbulence would not only be modelled, but would additionally be resolved and furthermore the speed of the calculations would decrease dramatically. The value of the smallest edge length of a refined cell was chosen to be 1.5mm for the presented investigations, which proved to be a good compromise between precision and speed for the given flow. The second aspect is the indicator value Φ_i in relation to the edge lengths h of the cells. The topological source of the flow, which is sensed by the refinement algorithm locally, might change its characteristics on a grid with better resolution. Thus the refined grid must always leave space for the detected topology to move, in contrast to forcing the flow into the automatically refined path. The more the topology develops during the succeeding stages of

adaptation, the less movement can be expected. The indicator-function I_e determines, if an edge e of a cell is worth of refining or not by comparing the indicator values of all cell edges over all domains (eq. 1). Since this function is a product of the indicator value Φ_i and the edge length h, its sensitivity can by modified by the h-scaling power α_e [8]. Thereby larger cells can be ranked higher in the gradient based indicator scheme. Cell cluttering and thus forcing the flow is avoided. Therefore the used set-up starts out at an α_e-value of 1.15 and is reduced towards 1.0 throughout the steps. For an additional fine tuning the indicator i can be weighted by the parameter C_i, which gives the user the means to create a fitting indicator scheme for almost any type of flow.

$$I_e(i) = C_i \frac{\Phi_{i,e}}{\Phi_{i,max}} h^{\alpha_e} \tag{1}$$

3.1 Numerical Set-Up

Even though the scope of this paper focusses on the design of a suitable combat aircraft planform in order to address aeroelastic phenomena in wind tunnel experiments a few words on the numerical set-up shall be made. The grid adaptation technique made the process of grid generation obsolete, except for the surface grid and the boundary layer grids. The edge length of the surface cells at the leading edges and the wing tip go down to 0.135mm in order to resolve the feeding sheet at the leading edge radius properly. The rest of the suction surface is covered with cells of 1mm edge length and of 5mm edge length at the pressure side (fig.1). Since the vorticity for the leading edge separation and the thereof developing vortices is generated mostly in the shear layer, such a precise surface resolution is needed as a stable base throughout the entire flight regime for this particular combat aircraft planform. The same accounts for the resolution of the boundary layer in the prism layer. The initial cell height was chosen to be 0.57μm, which leads to an $y+$-value of about 0.8 to 1.2 throughout all calculations despite the high velocities at the leading edges and underneath the jet-type vortices. The stretching-ratio of the layers was 1.4767 up to layer 7 and 1.25 up to layer 21, which results in an overall height of 0.66mm. This value is most likely smaller than the boundary layer on most locations, but catches the biggest amount of the small velocities therein. Since the grid adaptation technique is used, areas in need of a better boundary layer resolution on top of the fixed prism layer can claim more cells after the initial calculation.

Around the prism layer a tetrahedral mesh with a stretching-ratio of 1.8 was created, which provided enough cells to form the onset of primary vortices and in some flight cases even secondary vortices (fig.7). The current calculations were done in steady state, even though the validation of using the grid adaptation technique for unsteady calculations on this fighter aircraft model are progressing. A comparative preliminary study showed, that the one-equation turbulence model SA-neg is sufficient. Since there were no major benefits in using the two-equation model $k-\omega$-SST or a Reynolds Stress Model, these low fidelity calculations were conducted with the SA-neg model, as it is implemented in the DLR-TAU code. This will probably change, when high fidelity calculations become the scope of the wind tunnel experiment preparations.

4 VORTICAL FLOW TOPOLOGY

As mentioned before the aircraft model comprises a two stage vortex system. This was achieved by creating a planform with two pairs of leading edges in the same sweep magnitude each. The ogival nose and the 75° swept part of the diamond fillet develop a supersonic vortex lifting

system, when the normal Mach-numbers at the 45° swept main wing and at the 45° swept edge of the diamond reach the value of unity. The normal Mach-number depends on the free stream Mach-number, on the angle of incidence α, on the sweep angle λ and as well on the profile angle at the leading edge β':

$$Ma_n = M_\infty \sqrt{1 - \cos^2(\alpha - \beta') \sin^2 \lambda} \tag{2}$$

According to the theories of Polhamus, the leading edge separation subsides towards normal Mach-numbers around unity [9,10]. This process is gradual and results in strong changes of the pressure distribution on the suction side. The transition between the subsonic and supersonic votex system stretches especially on geometries with radii at the leading edges. With 1% of the total span the leading edge radii of the current model are relatively small, which reduces the effects of the radii on the transition. Nevertheless, already the numerical results show the onset of the transition far earlier than eq. 2 would define for an angle of incidence $\alpha = 5^\circ$ for example. The predicted free stream Mach-number by the equation in order to reach unity at the leading edges equals 1.41 for this angle (fig. 8).

Due to the sharp leading edges, the shear layers form the vortex system early on at low angles of attack. The three primary vortices of the subsonic system lie in the free stream direction at first, but with increasing angle of attack their positions vary greatly. All three vortices grow in strength and diameter with increasing angle of attack, and as a result they start to interact. The two inner vortices begin to intertwine, which leads to a stabilization of the diamond vortex by the nose vortex. This behaviour is similar to the vortex dynamics on classical double delta wings [11, 12]. In contrast to this effect acts the wing vortex rather independently. However, its high vorticity induces a further outboard movement of the intertwined vortex pair. Eventually the vortex breakdown position of the main wing vortex reaches the trailing edge first and shortly after the breakdown position of the intertwined vortex pair reaches the trailing edge as well. Whereas the subsonic vortex topology poses several possibilities for strong vortex interaction the supersonic topology is less likely to show much interaction, let alone intertwining. The onsets of the feeding sheets are geometrically further apart in the high velocity regime and high angles of attack, which could increase the vorticity, are not sensible in respect to the structural loads.

5 AEROELASTIC CHALLENGES

The overall aeroelastic aim of the studies on the combat aircraft configuration called ”devil”-model is to increase the knowledge on vortex induced loads. Prior DLR-projects and wind tunnel experiments featured a lambda-wing configuration with a constant leading edge sweep and a constant ratio of local leading edge radius to local chord length (fig.10). The results of the experiments and additional numerical calculations showed mechanisms of buffeting due to vortex breakdown and furthermore hysteresis effects during pitching motion as a consequence of the vortical lift system, as well as vortex shock interaction in the transonic flight regime [13, 14].

The experiments in the new DLR-project ”Diabolo” extend the velocity range and the complexity of the vortical flow topology. This introduces further possibilities for load changes and diverse hysteresis effects. The most obvious effects are probably the different types of buffeting, which are introduced by vortex breakdown. The breakdown position of the vortices varies in

streamwise direction by an amount of approximately 5% of the local chord length [12, 15–17]. Consequently buffeting by vortex breakdown starts, when the breakdown of the main wing vortex reaches the vicinity of the trailing edge. This position of the vortex breakdown will lead to strong aperiodic load changes at the rear, since the suction peak on the surface corresponds to the position of the vortex breakdown. With further increasing angle of attack the position of breakdown moves onto the main wing and continues to fluctuate there until reaching the leading edge, where the vortical flow eventually subsides. Parallel to this phenomenon evolves a similar process with the intertwined vortex pair. The frequencies, the amplitudes, the induced suction peaks and thereby the induced load changes occur at different magnitudes, which leads to complex buffeting characteristics (fig.9).

Besides the local fluctuations the overall paths and thus the suction peaks of the vortices vary throughout the flight regime. Consequently the load distribution and the leverage of the moments as well as the onset of the forces vary likewise. An additional displacement effect is introduced by the different sweep angles of the leading edges, which leads to the transition of the vortex system between subsonic and supersonic normal Mach-number for the lower swept edges. This transition is expected to generate severe load changes during pitching manoeuvres, since the transition process is believed to occur rather rapid than gradually under dynamic motion in contrast to incremental incidence changes. A further consequence could be intense hysteresis effects due to accelerated or delayed vortex system transitions.

As in the previous experiments the new wind tunnel test campaign will feature periodic and aperiodic pitching motions in order to force hysteresis effects between the motion and the resulting forces. Again, the different leading edge sweeps will have an impact on the hysteresis effects. Vortices of different strength, with different breakdown position and different leverage augment the experiments complexity significantly. The chances of structural excitation are increased and the load shifts are more severe than in the former experiments.

6 SUMMARY AND OUTLOOK

In order to proceed in the research on vortex induced loads a new combat aircraft configuration was designed. The planform of the configuration provides a two stage vortex system that enables controlled subsonic and supersonic flight. Hand in hand with the vortex system go complex load changes, which are introduced by buffeting and hysteresis effects. The combat aircraft configuration will be constructed as a semi span model, whose structural lay-out has begun already. The sensor placement on the wind tunnel model is aided by numerical simulations, as has been the entire design process. The numerical calculations could resolve various flow topologies such as secondary separations, tertiary separations and vortex breakdowns throughout the subsonic and supersonic flight regime for different angles of attack very precisely by the usage of the DLR-TAU grid adaptation technique.

While the wind tunnel model is being constructed and instrumented, further numerical studies will prepare the envelope of the wind tunnel test campaign. The next step is the design of a suitable peniche in connection with a variable stand-off. Additionally gaps in the coefficient matrices will be closed by consecutive calculations with various Mach-numbers and angles of incidence. Next to improving the overall usage of the grid-adaptation procedure it will be tried to implement the feature of unsteady grid adaptation, whose usage has already been demonstrated before. With this tool at hand, the forced pitching motion experiments could be set up very efficiently [18].

7 REFERENCES

[1] Luckring, J. M. (2002). Reynoldy number and leading-edge bluntness effects on a 65deg delta wing. In *40th AIAA Aerospace Sciences Meeting & Exhibit*.

[2] Henderson, W. P. (1976). Effects on wing leading edge radius and reynolds number on logitudinal aerodynamic characteristics of highly swept wing body configurations at subsonic speeds. Tech. rep., NASA.

[3] Kern, S. B. (1993). Vortex flow control using fillets on a double-delta wing. *Journal of Aircraft*.

[4] Hall, R. (1998). Impact of fuselage cross section on the stability of a generic fighter. In *16th AIAA Applied Aerodynamics Conference*.

[5] Cohen, D. and Jones, R. T. (2015). *High speed wing theory*. Princeton University Press.

[6] Alrutz, T. and Rütten, M. (2005). Investigation of vortex breakdown over a pitching delta wing applying the dlr tau-code with full, automatic grid adaptation. In *35th AIAA Fluid Dynamics Conference and Exhibit*.

[7] Fritz, W. (2007). Rans solutions for the cawapi f-16xl in solution adapted hybrid grids. In *45th AIAA Aerospace Sciences Meeting and Exhibit*.

[8] Alrutz, T. and Orlt, M. (2006). Parallel dynamic grid refinement for industrial applications. In *European Conference on Computational Fluid Dynamics*.

[9] Polhamus, E. C. (1996). A survey of reynolds number and wing geometry effects on lift characteristics in the low speed stall region. Tech. rep., NASA.

[10] Polhamus, E. C. (1971). Predictions of vortex-lift characteristics by a leading-edge suctionanalogy. *Journal of Aircraft*.

[11] Erickson, G. E. (1991). Wind tunnel investigation of the interaction and breakdown characteristics of slender wing vortices at subsonic, transonic, and supersonic speeds. Tech. rep., NASA.

[12] Hebbar, S. K., Platzer, M. F., and Li, F. H. (1993). A visualization study of the vortical flow over a double-delta wing in dynamic motion. *AIAA*.

[13] Wiggen, S. and Voß, G. (2014). Vortical flow prediction for the design of a wind tunnel experiment with a pitching lambda wing. *CEAS Aeronautical Journal*.

[14] Wiggen, S. (2015). Unsteady pressure distributions at the wind tunnel model of a pitching lambda wing with development of vortical flow. *Aerospace Science and Technology*.

[15] Verhaagen, N. G. (1983). An experimental investigation of the vortex flow over delta and double-delta wings at low speed. Tech. rep., Delft University of Technology.

[16] Verhaagen, N. G., Jenkins, L. N., Kern, S. B., et al. (1995). A study of the vortex flow over 76/40-deg double-delta wing. Tech. rep., NASA.

[17] Wiggen, S. (2014). Experimental results for vortex dominated flow at a lambda-wing with a round leading edge in steady flow. In *AIAA SciTech*.

[18] Gardner, A. D., Richter, K., and Rosemann, H. (2007). Simulation of oscillating airfoils and moving flaps employing the dlr-tau unsteady grid adaptation. In *New Results in Numerical and Experimental Fluid Mechanics VI*. Springer.

COPYRIGHT STATEMENT

8 FIGURES

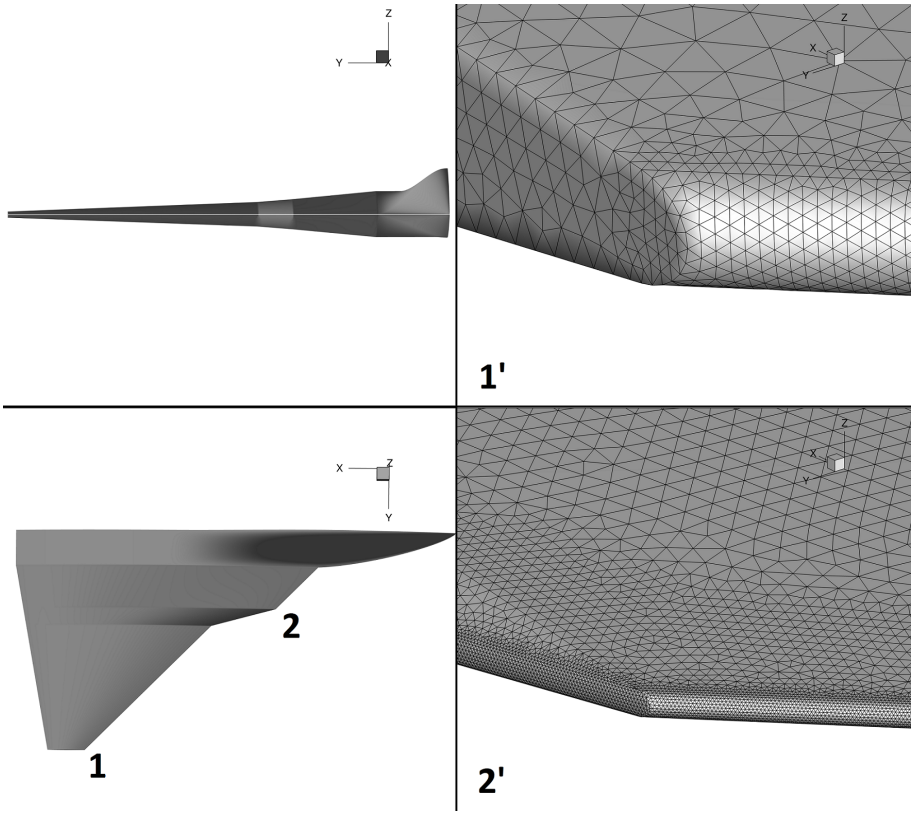

Figure 1: the semi-span fighter aircraft model and details on the grid resolution at the leading edges

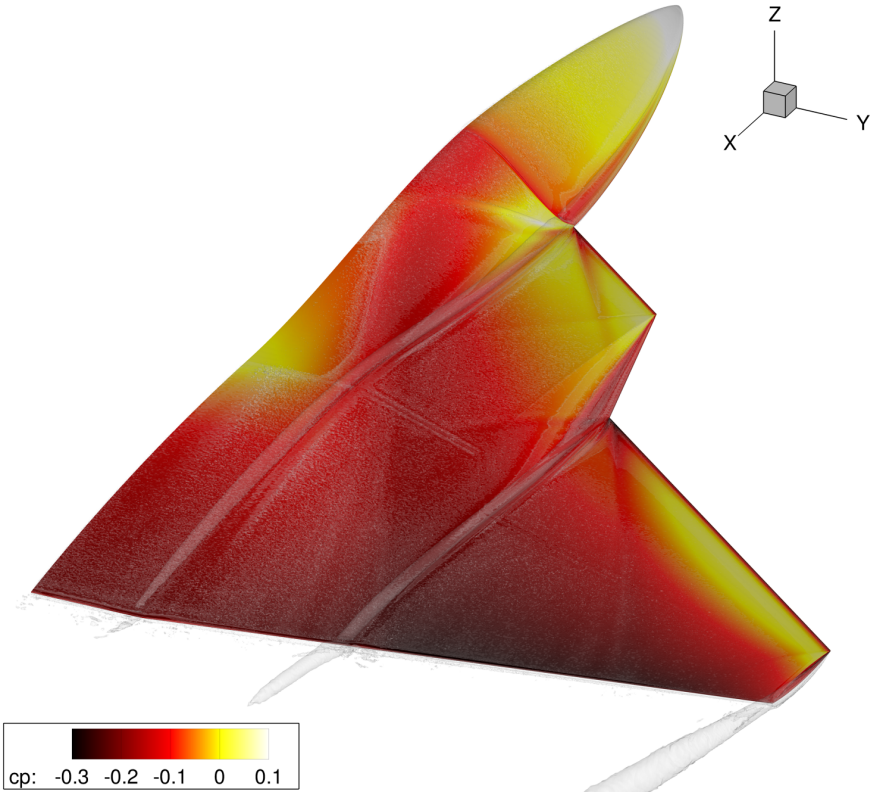

Figure 2: During acceleration towards higher Mach-numbers the second stage of the vortex system emerges. (visualized by Q-iso surfaces, $Ma = 1.8$, $\alpha = 5°$).

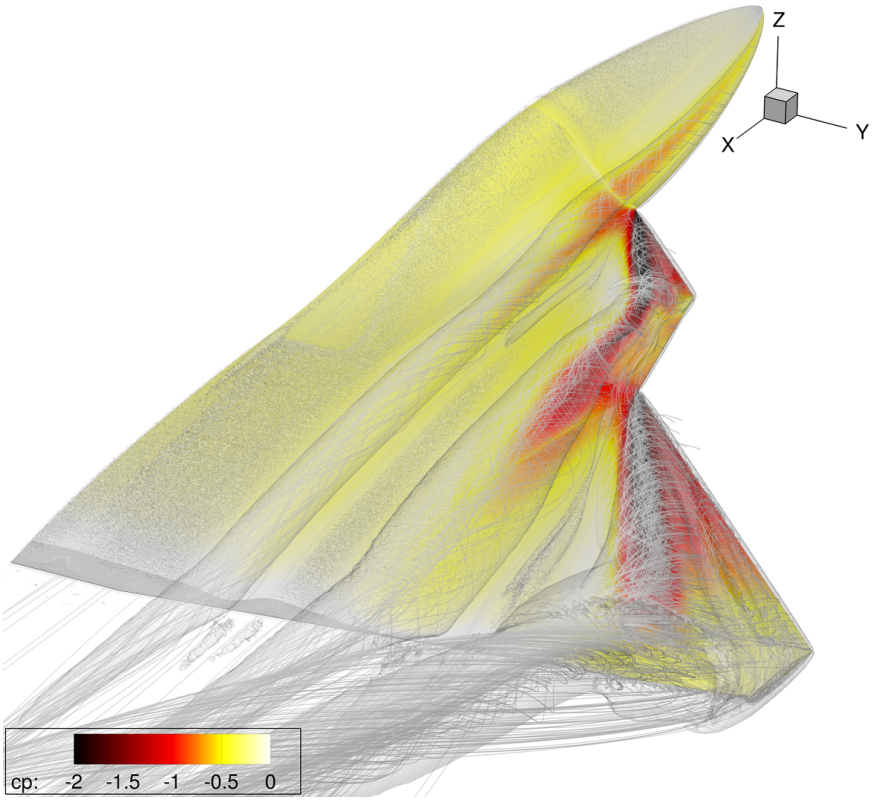

Figure 3: The three primary separations dominate the flow field in the subsonic flight regime. ($Ma = 0.5$, $\alpha = 10°$)

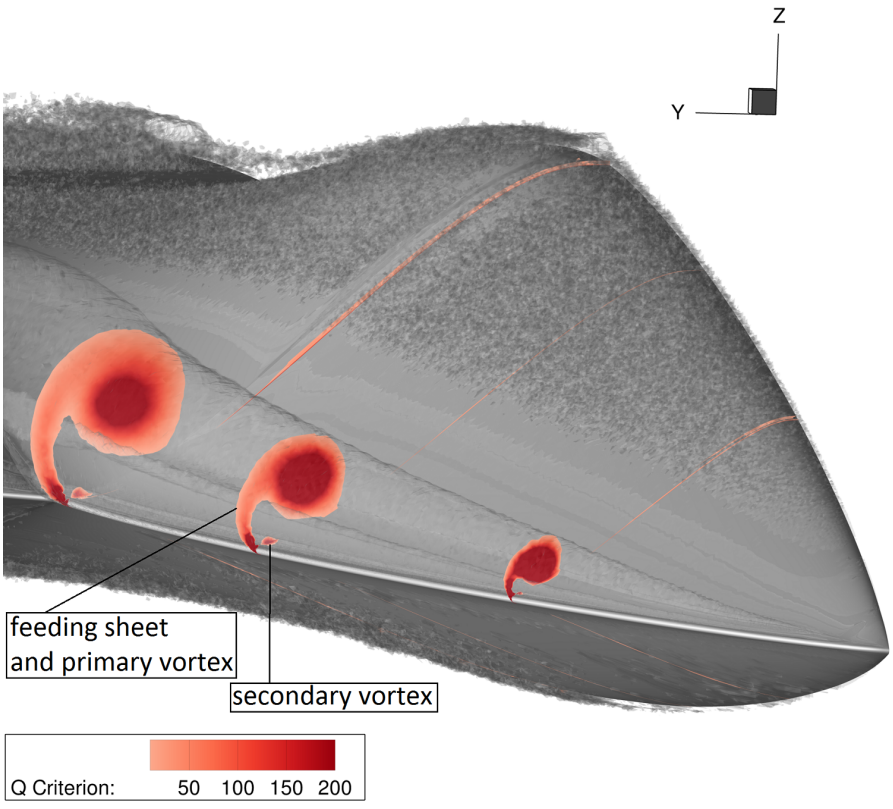

Figure 4: The cosine shaped chined nose creates a long living leading edge vortex.

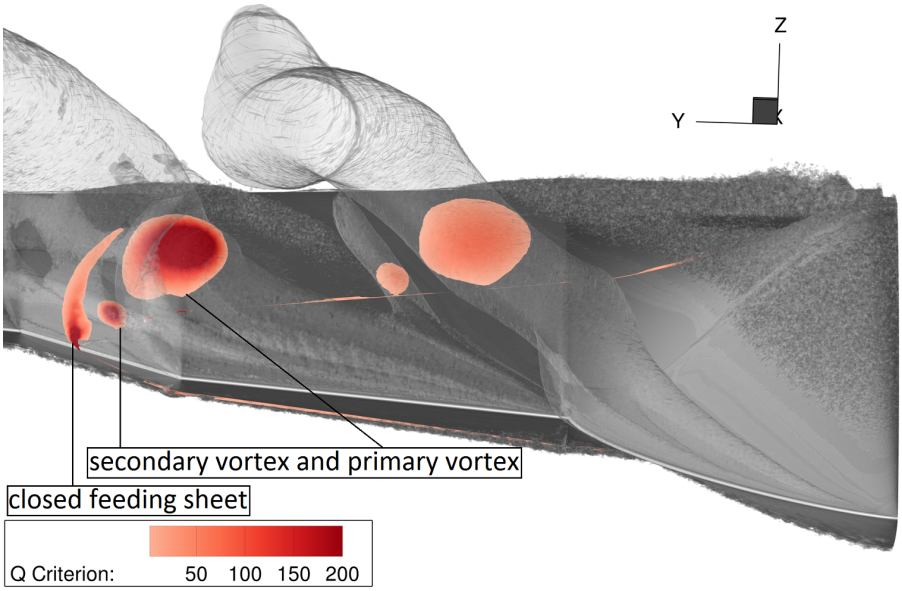

Figure 5: The diamond fillet creates a leading edge separation in subsonic as well as in supersonic flight.

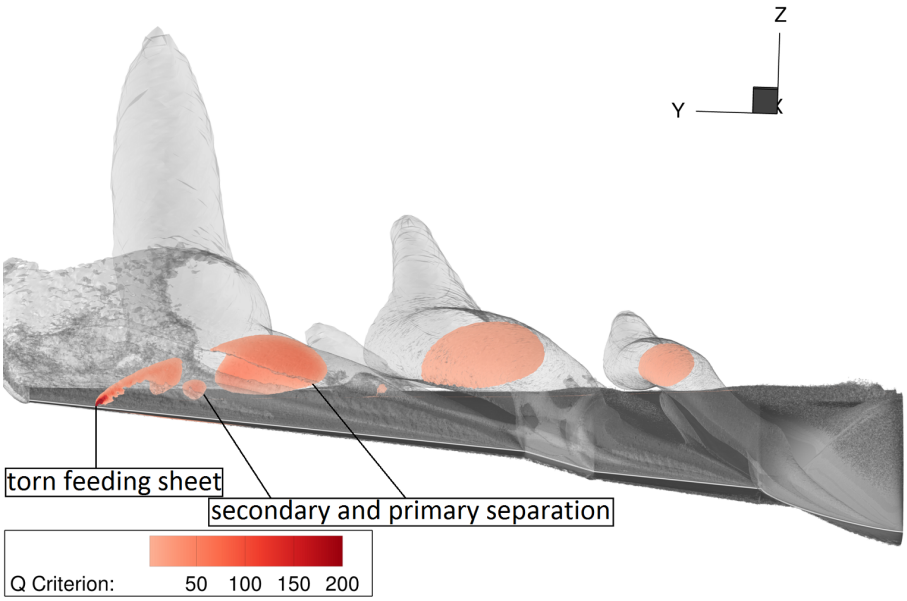

Figure 6: The wing vortex is not stabilized and feeding sheet tearing occurs throughout the flight regime.

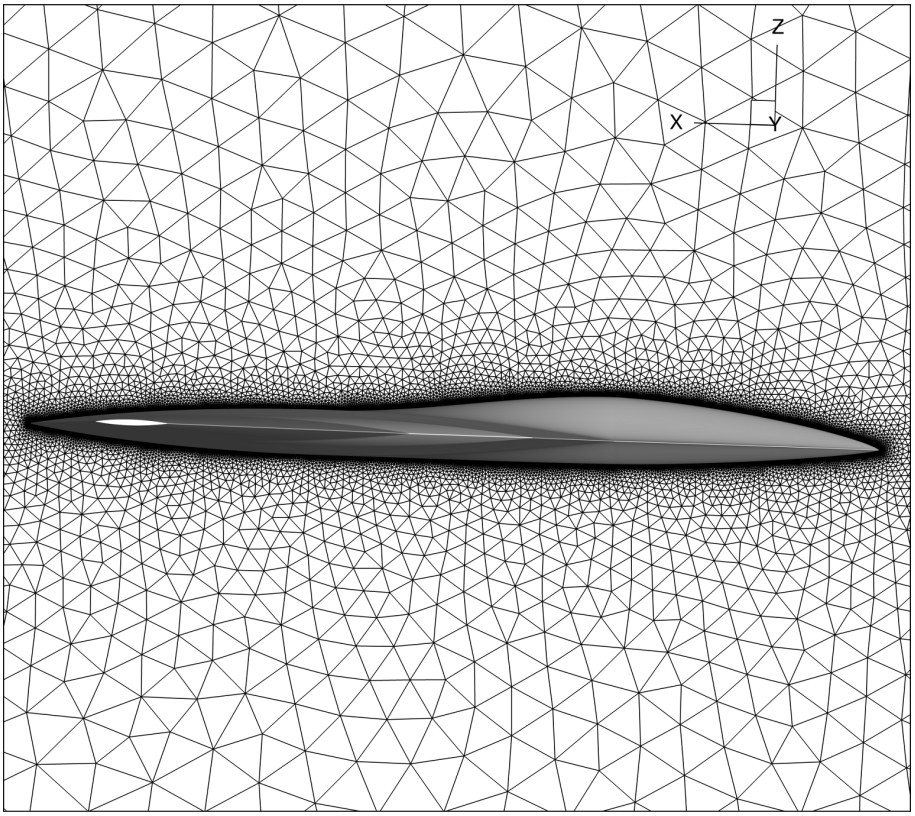

Figure 7: The fighter aircraft model is shown in its initial grid set-up as a semi-span configuration.

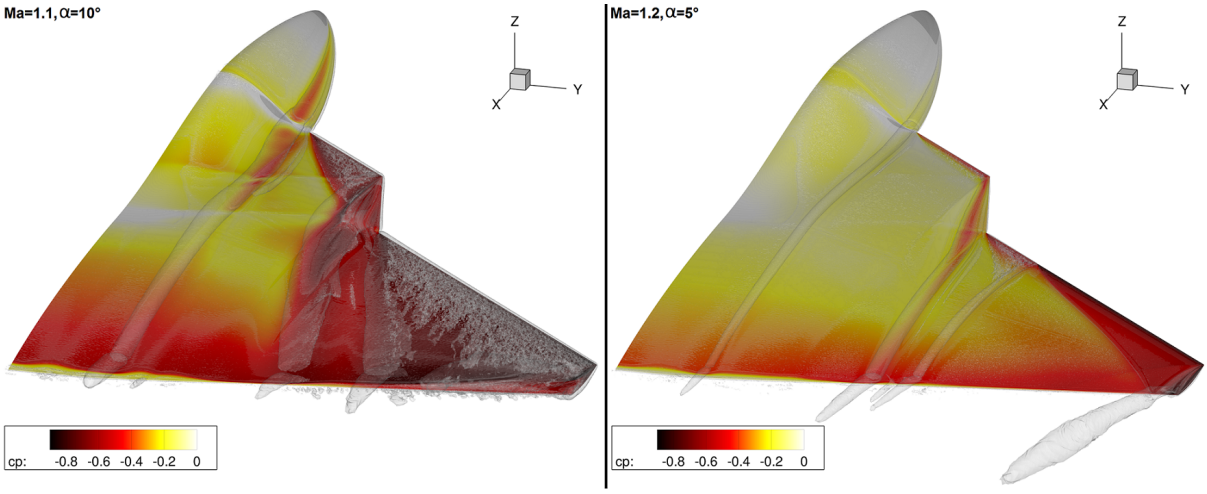

Figure 8: The transition between the two vortex systems occurs gradually (compare to fig. 2).

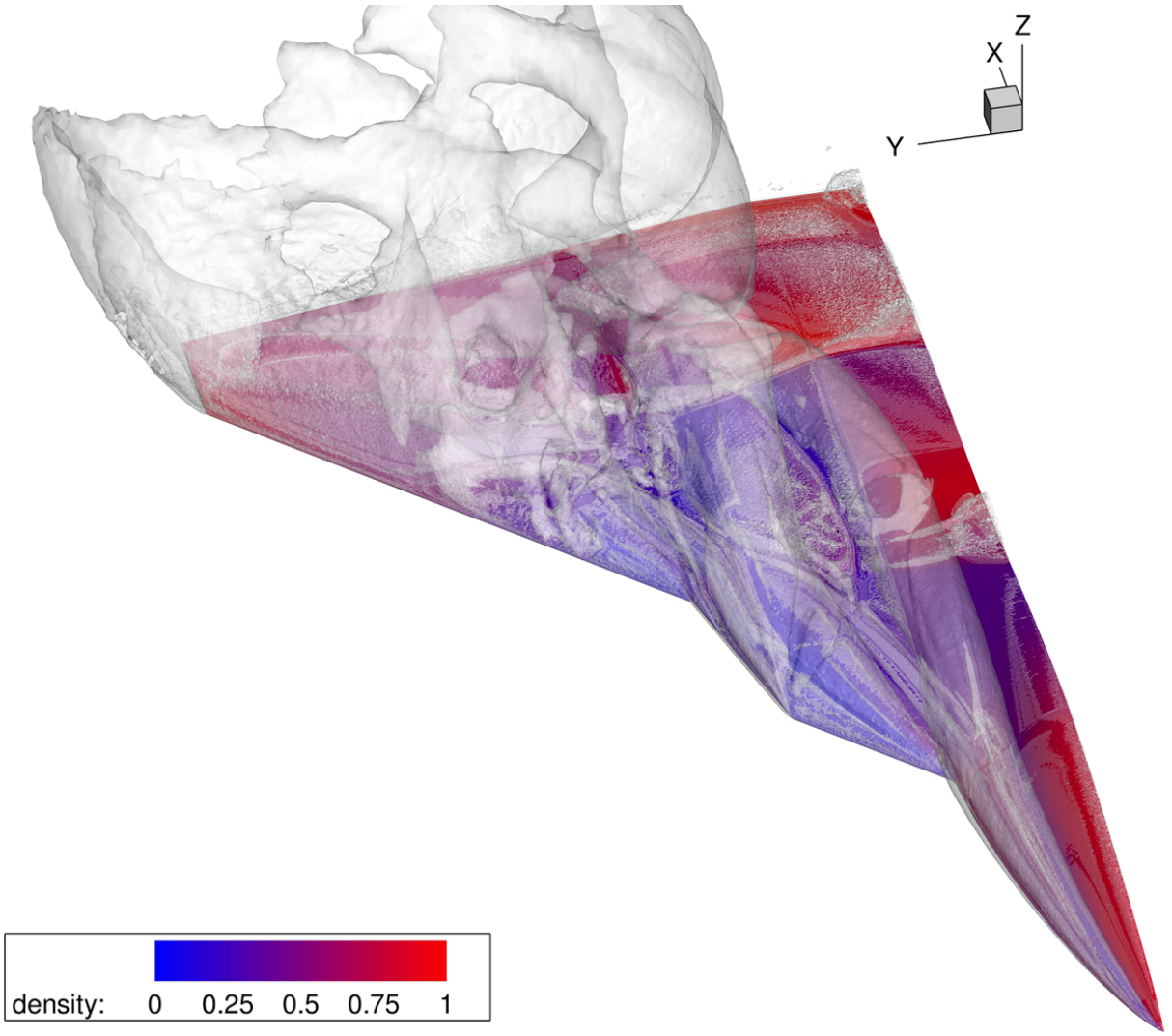

Figure 9: Next to vortex bursting and intertwining the occurrence of shocks raise further challenges for resolving the aerodynamic phenomena properly, which are relevant for aeroelastics. ($Ma = 0.85$, $\alpha = 25°$).

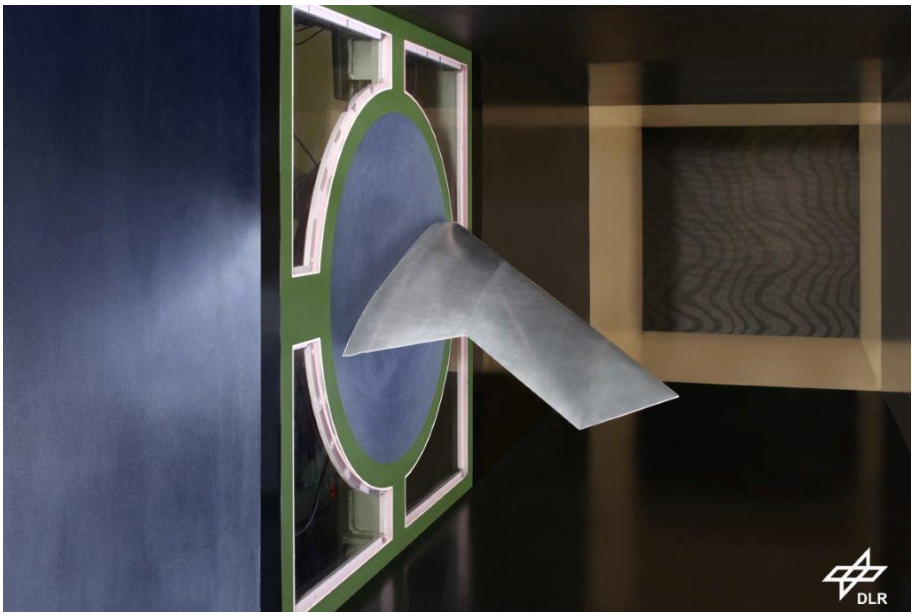

Figure 10: Lamda-wing model of the previous test campaign in the wind tunnel test section.